Available online at www.sciencedirect.com
SCIENCE DIRECT®
Colloids and Surfaces B: Biointerfaces 34 (2004) 191–196
COLLOIDS AND SURFACES B
www.elsevier.com/locate/colsurfb

Well-ordered self-assembled monolayer surfaces can be used to enhance the growth of protein crystals

Tan Pham, Denton Lai, David Ji, Wirote Tuntiwechapikul[1], Jonathan M. Friedman[2], T. Randall Lee*

Department of Chemistry, University of Houston, 4800 Calhoun Road, Houston, TX 77204-5003, USA

Accepted 13 January 2004

Abstract

A series of hydrophobic self-assembled monolayers (SAMs) was generated by the adsorption of undecanethiol, dodecanethiol, and octadecanethiol onto transparent gold-coated glass microscope slides. Protein crystallization trials using droplets deposited on the surfaces of the optically transparent SAMs were compared to those for which the droplets were deposited on the surfaces of conventional silanized glass microscope slides. For the five distinct proteins examined in the crystallization trials (i.e., lysozyme, α-lactalbumin, hemoglobin, thaumatin, and catalase), the SAMs generally afforded, (1) a faster rate of crystallization, (2) a larger crystal size; and (3) a broader range of crystallization conditions than that afforded by silanized glass. The greatest enhancements were observed with the highly ordered SAMs derived from octadecanethiol, which are evaluated here for the first time.

Keywords: Protein crystallization; Self-assembled monolayers; SAMs; Gold

1. Introduction

Protein structure determination remains an important and challenging tool in our efforts to understand fundamental biochemical pathways and to design new drugs. Currently, X-ray diffraction stands as the most widely used method for resolving protein structures in atomic detail [1]. While synchrotron X-ray sources allow for the analysis of protein crystals having small dimensions (e.g., $\leq$10 μm), access to appropriate synchrotron facilities can be limited. Conventional X-ray sources, on the other hand, require protein crystals having relatively large dimensions (e.g., 50–250 μm). In certain experimental situations (e.g., while working with fragile proteins and/or during the course of space-flight operations), protein crystals must be grown quickly. Given these considerations, many current research efforts are targeting the rapid growth of large protein crystals [2].

From the simplest perspective, there are three basic steps involved in protein crystallization: nucleation, propagation, and termination [1]. If nucleation is faster than propagation, then smaller crystals and/or amorphous precipitate can be expected. If, however, propagation is faster than nucleation, then large crystals can be expected as long as there is negligible or reversible formation of inhibitory macromolecular aggregates or non-productive precipitates. Hydrophobic polycarbonate and silanized glass surfaces are routinely used to support aqueous protein solutions in typical macromolecular crystallization devices, at least in part because hydrophobic surfaces cause aqueous droplets to "bead up" into nearly spherical geometries. Given that a sphere represents the three-dimensional shape with the lowest possible ratio of surface area to volume, the minimum surface area of the beaded drop gives rise to the slowest evaporation of water from the drop and thus the slowest approach to equilibrium. Although aqueous droplets spontaneously "bead up" on hydrophobic surfaces regardless of the degree of surface order, studies have shown that selective control over the solid phase (crystallization apparatus) in contact with

* Corresponding author.
E-mail addresses: trlee@uh.edu (T. Randall Lee), jonathan.friedman@fazix.com (J.M. Friedman).
[1] Department of Biochemistry, Faculty of Medicine, Chiang Mai University, 110 Intawaroros Road, Muang, Chiang Mai 50200, Thailand.
[2] Co-corresponding author.

0927-7765/$ – see front matter © 2004 Elsevier B.V. All rights reserved.
doi:10.1016/j.colsurfb.2004.01.003

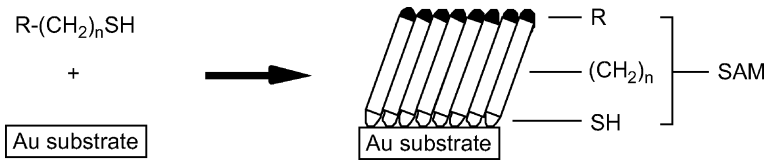

Fig. 1. Schematic illustrating the spontaneous formation of SAMs on gold.

the liquid phase (protein solution) can provide enhanced control of protein crystallization [3,4].

Based on these and related studies, we have been exploring the growth of protein crystals by vapor diffusion from aqueous droplets deposited onto the surfaces of well-defined self-assembled monolayers (SAMs) [5]. As shown in Fig. 1, SAMs can readily be formed by the spontaneous adsorption of ω-terminated alkanethiols onto the surface of gold [6]. These thin films have been widely used to tailor the surface properties of various substrates, including those used for the crystallization of minerals [7,8], amino acids [9], and other organic molecules [10]. In our previous investigation [5], we reported general enhancements in the rate of crystallization, the size of the crystals, and the range of crystallization conditions when aqueous protein droplets were placed in contact with optically transparent SAM-coated glass microscope slides rather than conventional silanized microscope slides. The results were found to be ubiquitous for a variety of proteins (i.e., lysozyme, α-lactalbumin, thaumatin, ribonuclease, hemoglobin, and catalase) deposited onto SAMs having a variety of ω-termini (R = CH_3, CH_2OH, COOH, and 2-imidazole). Based on the experimental data, we concluded that the enhancements afforded by the SAMs arose from an inhibition in the irreversible formation of non-productive amorphous precipitate (i.e., surfaces that were passivated by SAMs appeared to offer fewer sites for the nucleation of non-productive amorphous precipitate).

To test this hypothesis further, we report herein studies of protein crystal growth using aqueous protein droplets deposited on a series of CH_3-terminated SAMs for which the length of the alkyl chain of the thiol adsorbate is varied across 11, 12, and 18 carbon atoms. Previous studies of SAMs have established that a stepwise variation in the chain lengths (e.g., odd vs. even numbers of carbon atoms) gives rise to subtle structural differences at the exposed interfaces [11,12]. Moreover, several studies have established that SAMs having long chain lengths (e.g., 18 carbon atoms) exhibit markedly enhanced conformational order when compared to SAMs having progressively shorter chain lengths [6,12–14]. Given these considerations, we chose to examine the crystallization of a series of various proteins using the hanging-drop method in which the droplets are deposited on the surfaces of SAMs derived from $CH_3(CH_2)_{10}SH$ (undecanethiol; **C11**), $CH_3(CH_2)_{11}SH$ (dodecanethiol; **C12**), and $CH_3(CH_2)_{17}SH$ (octadecanethiol; **C18**). The results of these trials are then compared to analogous crystallization trials in which the protein droplets are deposited on the surfaces of conventional, commercially available silanized glass (**SG**). Representative crystallization profiles are presented in Fig. 2; selected data are further highlighted in Table 1 and discussed in the following paragraphs.

2. Materials and methods

2.1. Reagents

Undecanethiol, dodecanethiol, and octadecanethiol were obtained in the highest purity available from Aldrich Chemical Company. Ultrahigh purity gold shot (99.99%) was purchased from Americana Precious Metals, and polyethyleneglycol-4000 (PEG-4000) was purchased from Fluka Chemical Company. Unmodified glass coverslips were obtained from Fischer Scientific, while silanized glass coverslips were obtained from Hampton Research. Hen egg lysozyme, bovine α-lactalbumin, horse hemoglobin, thaumatin, and bovine liver catalase were purchased from commercially available sources and purified according to procedures described in the literature [15].

2.2. Preparation of gold-coated glass coverslips

Glass coverslips were sonicated three times each in soap (Alconox) solution, purified water, and absolute ethanol, respectively, and blown dry with ultrapure nitrogen. Gold substrates were prepared by initially evaporating 2.5 nm of chromium (to promote the adhesion of gold), followed by 15 nm of gold onto unmodified glass coverslips.

2.3. Preparation and analysis of SAMs

The freshly prepared gold-coated glass coverslips were immersed in ethanolic solutions of the respective alkanethiols for 24 h. The quality of the SAMs was evaluated by spot checks of the advancing contact angle of hexadecane on the SAMs using a ramé-hart model 100 contact angle goniometer. For each type of SAM, the value of the contact angle was averaged from measurements on four distinct gold-coated glass coverslips.

2.4. Crystallization trials

The vapor-diffusion method at room temperature (∼22 °C) was employed for all crystallization trials in standard Linbro trays. The 4 μl protein droplets were sealed above wells containing a series of selected precipitant

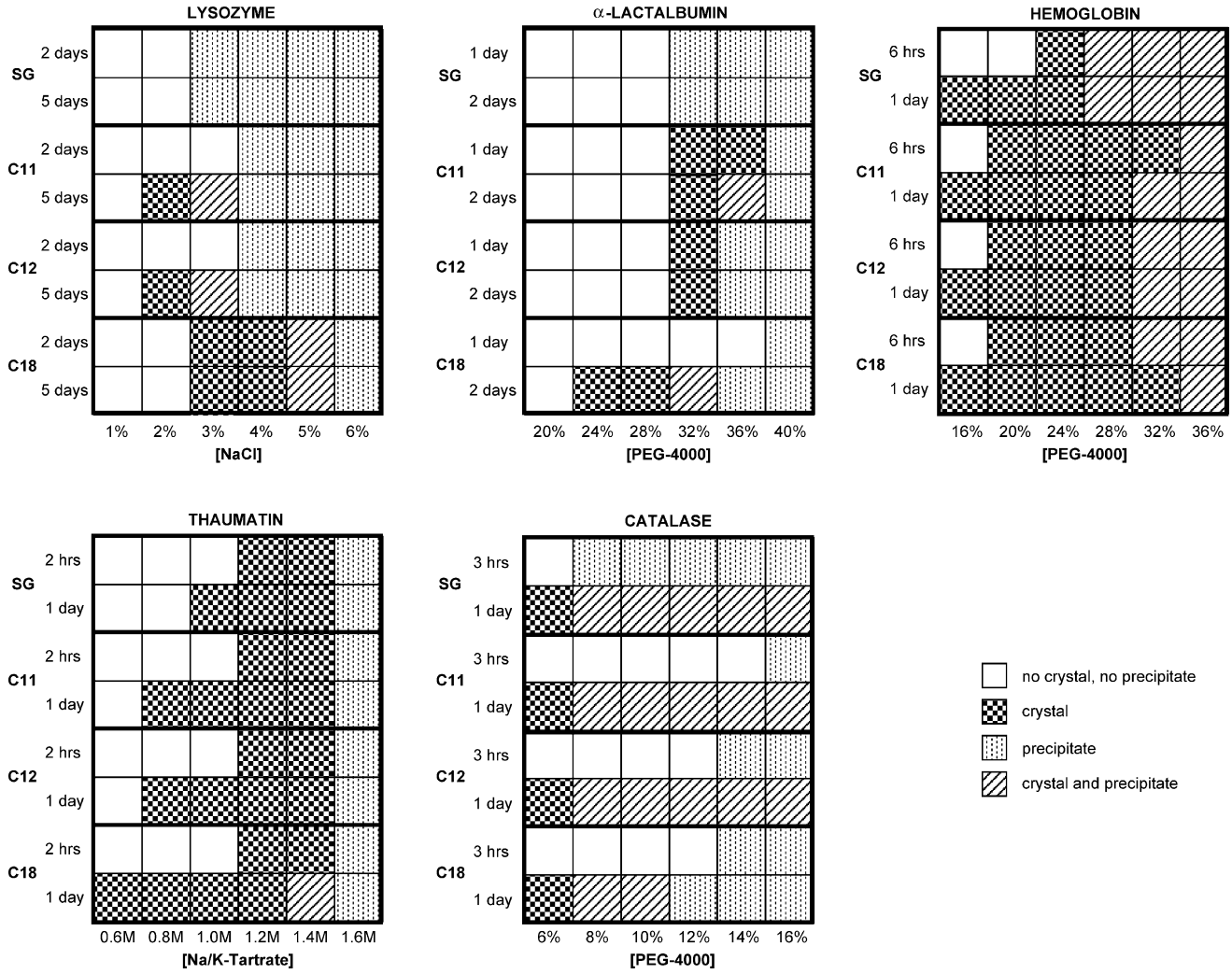

Fig. 2. Selected crystallization profiles on the various surfaces (**SG**, **C11**, **C12**, and **C18**). The volume of each protein-containing droplet was 4 μl, and the volume of precipitant solution in each well was 1 ml. All proteins were dialyzed against their initial buffer solution: lysozyme (0.1 M acetate, pH 4.8); α-lactalbumin (0.1 M Tris–HCl, pH 8.5); hemoglobin (0.1 M sodium phosphate, pH 6.5); thaumatin (0.1 M MOPS, pH 6.8); catalase (0.03 M sodium phosphate, pH 6.1).

Table 1
Summary of the data from the crystallization trials

Protein and initial conc.	Initial precipitate formation[a]	Initial crystal formation[a]	Largest crystal formation[b]
Lysozyme 35 mg/ml	2 days on **SG** surface At 3% (w/v) NaCl	2 days on **C18** surface At 3% (w/v) NaCl	2 days on **C18** surface At 3% (w/v) NaCl
α-Lactalbumin 45 mg/ml	1 day on **SG** surface At 32% (w/v) PEG-4000	1 day on **C11**, **C12** surface At 32% (w/v) PEG-4000	2 days on **C18** surface At 24% (w/v) PEG-4000
Hemoglobin 35 mg/ml	6 h on **SG** surface At 28% (w/v) PEG-4000	6 h on all SAMs At 20% (w/v) PEG-4000	6 h on **C18** surface At 20% (w/v) PEG-4000
Thaumatin 35 mg/ml	2 h on all surfaces At 1.6 M Na/K-tartrate	2 h on all surfaces At 1.2 M Na/K-tartrate	2 days on **C11** surface At 0.8 M Na/K-tartrate
Catalase 2.5 mg/ml	3 h on **SG** surface At 8% PEG-4000	1 day on all surfaces At 6% (w/v) PEG-4000	1 day on **C18** surface At 6% PEG-4000

[a] These data reflect the shortest time interval and the lowest precipitant concentration at which crystals or precipitate were observed to form.
[b] These data reflect the comparison in size of crystals at the shortest time when large crystals (>0.5 mm in diameter) were first observed to form. The volume of each protein-containing droplet was 4 μl. The volume of precipitant solution in each well was 1 ml. All proteins were dialyzed against their initial buffer solution: lysozyme (0.1 M sodium acetate, pH 4.8); α-lactalbumin (0.1 M Tris–HCl, pH 8.5); hemoglobin (0.1 M sodium phosphate, pH 6.5); thaumatin (0.1 M MOPS, pH 6.8); catalase (0.03 M sodium phosphate, pH 6.1). **SG**: silanized glass. **C11**, **C12**, and **C18** are SAMs derived from undecanethiol, dodecanethiol, and octadecanethiol, respectively.

concentrations. Crystallization data for each type of protein droplet on each type of surface at the selected precipitant concentrations were collected at progressive incubation intervals (up to 5 days unless stated otherwise). Crystal shape, size, and the number of crystals were also recorded. The crystal size was defined as small if the size was between 0.1 and 0.2 mm, medium if the size was between 0.2 and 0.5 mm, and large if the size was >0.5 mm. Additional experimental details can be found in Section 3, the figure captions, and in Table 1.

3. Results

The objective of this study was to evaluate the influence of surface conformational order on the growth of protein crystals. Measurements of the contact angle of hexadecane represent one of the most sensitive tools for evaluating the conformational order of hydrocarbon thin films [6]. High hexadecane contact angles ($\geq 50^\circ$) are observed on hydrocarbon SAMs only when the monolayers are densely packed and highly crystalline [12–14]. On the SAM-modified coverslips, we found the averaged values of the hexadecane contact angle to be 37, 45, and 50°, respectively, for the SAMs derived from undecanethiol (**C11**), dodecanethiol (**C12**), and octadecanethiol (**C18**). The values reported here are comparable to those reported for these same SAMs on glass microscope slides coated with a more traditional thick (1000 Å) layer of gold [13]. The contact angle values increase with increasing chain length because interfacial gauche defects in the SAMs progressively diminish due to the increasing interchain van der Waals stabilization that is concomitant with an increase in chain length [14]. We also measured the hexadecane contact angle of the commercially available silanized glass (**SG**) coverslips; the averaged value was only 13°. These data provide strong evidence that the surfaces of the **C18**-coated coverslips are more conformationally ordered than those modified with **C11** or **C12**, and substantially more ordered than the surface of commercially available **SG** coverslips.

Fig. 2 summarizes our experimental observations of the protein crystallization trials on the various surfaces (**SG**, **C11**, **C12**, and **C18**) at selected concentrations of precipitant. Table 1 shows the time and conditions of initial crystal formation, initial precipitate formation, and the largest crystal formation. Detailed descriptions of these protein crystallization trials are provided in the following paragraphs.

3.1. Lysozyme

These crystallization trials were performed using hanging drops of lysozyme solution (4 μl drop at 35 mg/ml) sealed above a series of wells containing selected concentrations of precipitant (1–6% (w/v) NaCl). Throughout the duration of the experiments (5 days), crystals in the form of tetragonal pyramids were observed to form under the broadest range of conditions for **C18** > **C12**–**C11** > **SG**. Crystals were first observed on the **C18** surface after 2 days at NaCl concentrations ranging from 3 to 4% (w/v). After 5 days at a NaCl concentration of 2% (w/v), crystals were also observed on the **C11** and **C12** surfaces. Crystals failed, however, to form in any of the trials using the **SG** surface. Qualitatively, the largest crystals were observed on the **C18** surface (see Table 1). With regard to precipitation, we observed the formation of precipitate under a wider range of conditions for **SG** > **C**11–**C**12 > **C**18.

3.2. α-Lactalbumin

These crystallization trials were performed using hanging drops of α-lactalbumin solution (4 μl drop at 45 mg/ml) sealed above a series of wells containing selected concentrations of precipitant (20–40% (w/v) PEG-4000). Crystals in the form of elongated slabs were first observed after 1 day on the **C11** surface at PEG-4000 concentrations of 32 and 36% (w/v), and on the **C12** surface at a PEG-4000 concentration of 32% (w/v). Crystals were also observed after 2 days on the **C18** surface, but at lower PEG-4000 concentrations (24–28% (w/v)). Although no crystals were observed in any of the trials using the **SG** surface after 2 days, a sprinkling of crystals was observed after 6 days. The general trends in crystallization after 6 days of incubation are highlighted by the images in Fig. 3. Although crystals were observed sooner on the **C11** and **C12** SAMs than on the **C18** SAM, the latter crystals grew larger and more uniformly shaped than the former crystals (see Fig. 3 and Table 1). With regard to precipitation, we observed the formation of precipitate after 1 day on the **SG** surface over a broad range of PEG-4000 concentrations (32–40% (w/v)) but on the SAM surfaces only at the highest PEG-4000 concentration (40% (w/v)).

3.3. Hemoglobin

These crystallization trials were performed using hanging drops of hemoglobin solution (4 μl drop at 35 mg/ml) sealed above a series of wells containing selected concentrations of precipitant (16–36% (w/v) PEG-4000). Crystals in the form of monohedra were observed under the broadest range of conditions for **C18**–**C12**–**C11** > **SG**. The crystals were observed on all three SAM surfaces after 6 h at PEG-4000 concentrations ranging from 20 to 36% (w/v). In contrast, crystals were observed to form on the **SG** surface after 6 h at PEG-4000 concentrations ranging from 24 to 36% (w/v). Meanwhile on the SAM surfaces, precipitate formed only at the highest PEG-4000 concentrations (32 and 36% (w/v)). In contrast, precipitate was observed to form on the **SG** surface over a wider range of PEG-4000 concentrations (28–36%). In general for all surfaces, an increase in the PEG-4000 concentration led to more numerous but markedly smaller crystals. Again, the **C18** surface afforded the largest and most uniform crystals when compared with the other surfaces under the same conditions (see Table 1).

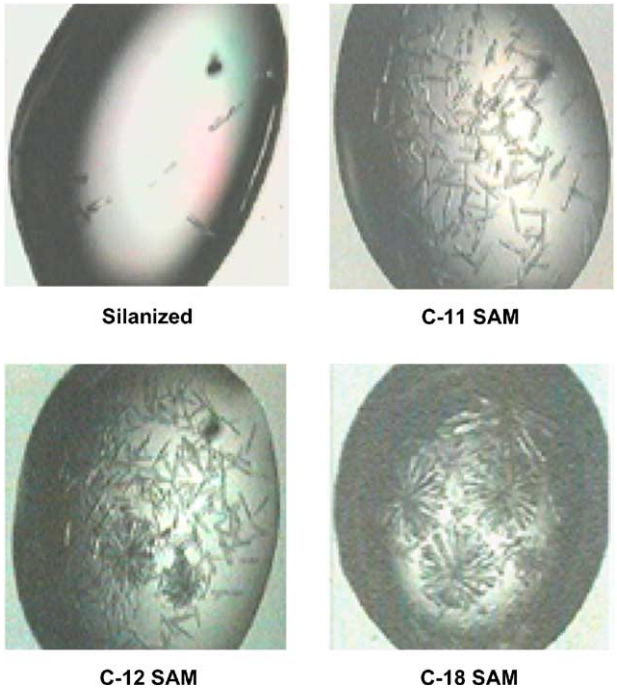

Fig. 3. Optical photographs of selected droplets illustrating the crystallization behavior of α-lactalbumin on the **SG**, **C11**, **C12**, and **C18** surfaces after 6 days at a PEG-4000 concentration of 24% (w/v). For **C18**, surface nucleation has slowed to the point where nucleation from a pre-formed crystallite is faster than nucleation at the surface, which leads to the growth of larger crystals. In general, more and larger crystals were observed on the SAM surfaces, with the greatest enhancements observed using the **C18** surface.

3.4. Thaumatin

These crystallization trials were performed using hanging drops of thaumatin solution (4 μl drop at 35 mg/ml) sealed above a series of wells containing selected concentrations of precipitant (0.6–1.6 M Na/K-tartrate). Crystals in the form of tetragons were observed to form under the broadest range of conditions for **C18** > **C12**–**C11** > **SG**. The onset of crystallization occurred on all surfaces after 2 h at Na/K-tartrate concentrations of 1.2 and 1.6 M. Similarly, precipitate was observed after 2 h on all surfaces at the highest Na/K-tartrate concentration employed (1.6 M). Qualitatively, the largest crystals were observed on the **C11** SAM after 2 days at a Na/K-tartrate concentration of 0.8 M (Table 1).

3.5. Catalase

These crystallization trials were performed using hanging drops of catalase solution (4 μl drop at 2.5 mg/ml) sealed above a series of wells containing selected concentrations of precipitant (6–16% (w/v) PEG-4000). Crystals in the form of rectangular prisms were first observed after 1 day on all surfaces at the lowest concentration of precipitant (6% PEG-4000). Qualitatively, although crystals were observed on all surfaces at the lowest PEG-4000 concentration (6% (w/v)), the **C18** surface afforded both the most crystals and the largest crystals. After 3 h of incubation on the **SG** surfaces, we observed the formation of precipitate under most of the conditions studied; in contrast, after 3 h of incubation on the SAM surfaces, we observed the formation of precipitate only at the highest precipitant concentrations (14 and 16% (w/v) PEG-4000). After 1 day of incubation, however, the formation of precipitate was commonly observed even on the SAM surfaces.

4. Discussion

From an overall perspective, the data collected here show that SAM surfaces offer distinct enhancements in protein crystallization when compared to conventional silanized glass surfaces. Furthermore, the data are consistent with a model in which these enhancements arise from a reduction in nucleation at the solution–surface interface, which allows crystallization to proceed at protein concentrations in excess of those that can be used in the absence of well ordered SAMs. In particular, we observe that SAM surfaces can inhibit the rate and reduce the amount of amorphous precipitate formation. With only a few exceptions, these trends are amplified when using the **C18** SAM.

Although past studies have demonstrated that certain well-ordered surfaces can offer uniform productive nucleation sites that promote crystal growth, we feel that a different phenomenon is at work here given that low free energy CH_3-terminated SAMs are likely to provide little kinetic or thermodynamic incentive for crystal nucleation. Moreover, given that **C18** SAMs are more highly ordered and defect-free than shorter chain analogs such as **C11**, **C12**, and related silanized surfaces [16,17], we propose that the SAM surfaces exert their influence by inhibiting the rate of non-productive nucleation (i.e., the formation of inhibitory macromolecular aggregates or non-productive precipitates) relative to the rate of productive nucleation (i.e., crystal formation). Indeed, separate studies have shown that amorphous nucleation is promoted by disordered interfaces, such as those afforded by mica and silanized glass [18]. An inhibition in the formation of amorphous precipitate would maximize the concentration of protein in solution, which in turn would maximize the rate of crystallization and/or the size of the resultant crystals.

5. Conclusions

In summary, crystallization studies of lysozyme, α-lactalbumin, hemoglobin, thaumatin, and catalase have demonstrated that SAM surfaces can be used to enhance: (1) the rate of crystallization, (2) the size of crystals formed, and (3) the range of crystallization conditions when compared to conventional, commercially available silanized glass surfaces. Moreover, both the rate of formation and the amount

of amorphous precipitate were generally less on the SAMs than on silanized glass. The effects were, in general, most pronounced for the most highly ordered **C18** SAM surfaces, which are evaluated here for the first time. We conclude that the enhancements afforded by the SAM surfaces arise from a decrease in the rate of non-productive nucleation relative to the rate of productive crystal formation.

Acknowledgements

This research was generously supported by the National Aeronautics and Space Administration (NRA-96-OLMSA-03) and the Robert A. Welch Foundation (E-1320).

References

[1] Z. Kam, H.B. Shore, G. Feher, J. Mol. Biol. 123 (1978) 539.
[2] A. McPherson, A.J. Malkin, Y.G. Kuznetsov, S. Koszelak, M. Wells, G. Jenkins, J. Howard, G.J. Lawson, J. Crystal Growth 196 (1999) 572.
[3] A. McPherson, P. Shlichta, Science 239 (1988) 385.
[4] S.A. Hemming, A. Bochkarev, A.D. Seth, R.D. Kornberg, P. Ala, D.S.C. Yang, A.M. Edwards, J. Mol. Biol. 246 (1995) 308.
[5] D. Ji, C.M. Arnold, M. Graupe, E. Beadle, R.V. Dunn, M.N. Phan, R.J. Villazana, R. Benson, R. Colorado Jr., T.R. Lee, J.M. Friedman, J. Crystal Growth 218 (2000) 390.
[6] A. Ulman, Characterization of Organic Thin Films, Butterworth–Heinemann, Boston, 1995.
[7] Y.-J. Han, J. Aizenberg, J. Am. Chem. Soc. 125 (2003) 4032.
[8] B. Krisanu, K. Vijayamohanan, Langmuir 14 (1998) 6924.
[9] A.Y. Lee, A. Ulman, A.S. Myerson, Langmuir 18 (2002) 5886.
[10] L.M. Frostman, M.M. Bader, M.D. Ward, Langmuir 10 (1994) 576.
[11] M. Graupe, M. Takenaga, T. Koini, R. Colorado Jr., T.R. Lee, J. Am. Chem. Soc. 121 (1999) 3222.
[12] Y.-S. Shon, S. Lee, R. Colorado Jr., S.S. Perry, T.R. Lee, J. Am. Chem. Soc. 122 (2000) 7556.
[13] W.J. Miller, N.L. Abbott, Langmuir 13 (1997) 7106.
[14] P.E. Laibinis, G.M. Whitesides, D.L. Allara, Y.-T. Tao, A.N. Parikh, R.G. Nuzzo, J. Am. Chem. Soc. 113 (1991) 7152.
[15] A. McPherson, Crystallization of Biological Macromolecules, Cold Spring Harbor Laboratory Press, New York, 1998.
[16] C.D. Bain, G.M. Whitesides, J. Am. Chem. Soc. 110 (1988) 3665.
[17] S. Wasserman, Y.-T. Tao, G.M. Whitesides, Langmuir 5 (1989) 1074.
[18] A. Schaper, Y. Georgalis, P. Umbach, J. Raptis, W.J. Saenger, Chem. Phys. 106 (1997) 8587.